International Journal of Latest Engineering and Management Research (IJLEMR)
ISSN: 2455-4847
www.ijlemr.com Volume 1 Issue 2 ǁ March 2016 ǁ PP.10-21

Improved photocatalytic performance of graphene supported sulfated nanoTiO_2

P. Mohapatra [1*] and K. M. Parida[2]
[1] Department of Chemistry, C.V. Raman College of Engineering, Bidyanagar, Mahura, Janla, Bhubaneshwar 752054, Odisha, India
2 Department of Chemistry, SOA University, Bhubaneswar-751 030, Odisha-India

ABSTRACT: To find out the effect of sulfate modification on the photocatalytic activity of nano TiO_2 (prepared by acid hydrolysis of tetraisopropyl orthotitanate), it was promoted with 2.5 wt.% sulfate by impregnation method using dilute H_2SO_4 as the precursor. The sulfate modification reduces the particle size and other morphological properties of nano sized TiO_2. Sulfation process also stabilizes the anatase phase of TiO_2 up to 873K. The photocatalytic activities of the sulfated nano TiO_2 catalysts were evaluated by performing different photocatalytic reactions such as decomposition 4-nitrophenol (organic pollutant), reduction of Cr(VI) (inorganic pollutant) and decolorization of methylene blue (dye pollutant). It was observed that the anchored SO_4^{2-} improves the visible light photocatalytic activity of TiO_2 by suppressing the recombination of electrons and holes. Graphene supported sulfated nano TiO_2 was prepared by varying the amount of graphene and evaluated for the photoreduction of Cr(VI). We observed improved photocatalytic activity for the graphene supported sulfated nano TiO_2 photocatalyst towards the reduction of Cr(VI). The percentage of photoreduction of Cr(VI) over 5wt% graphene supported sulfated nano TiO_2 was 99% where as it was 79% for sulfated nano TiO_2.

KEYWORDS: Degradation, Graphene, Photocatalyst, Sulphated nano TiO_2, Visible light

1. INTRODUCTION

Semiconductor photocatalysis has attracted much attention towards the environmentally important reactions. TiO_2 is the most investigated semiconductor photocatalyst and has been widely studied during the past decade [1–11]. It has been extensively used in environmental applications due to its nontoxicity, photostability, low cost, and water insolubility under most conditions. Since, TiO_2 is photoactive under UV irradiation; efforts have been made to modify it by different methods so that it responds to visible light. The sulfated TiO_2 solid acid has been introduced as a photocatalyst for its higher catalytic activity compared to neat TiO_2 in the photodegradation of some organic compounds [12-14]**.** Furthermore, the surface acidic property of SO_4^{2-}/TiO_2 catalyst considered important for the enhancement of photocatalytic activity. It is generally assumed that co-ordinatively unsaturated Ti^{4+}sites may act as the Lewis acidic sites on both TiO_2 and sulfated TiO_2. After sulfation, new Brønsted acid sites can be generated on the metal oxide though their detailed structures are not known [15]. These acid sites are believed to be capable of increasing the adsorption of organic pollutions and capturing the photoinduced electrons more effectively, which leads to an increase in the quantum yield [16-17]. Sulfation of TiO_2 hinders the particle growth, which in turns prevents the agglomeration of particles during the synthesis, so the particle size reduces. The sulfated nano TiO_2 particles absorb in the visible region of the solar spectrum, thereby makes it suitable for the application in the water treatment methods using direct solar radiation.

At present graphene has been widely studied for use in various applications such as electronic and optoelectronic devices, supercapacitors, and chemical sensing, etc due to its excellent electrical, optical, mechanical, and thermal properties [18–22]. More recent studies have been concentrated on the synthesis and applications of graphene modified photocatalyst because their large specific surface area and high activity in most of the catalytic processes. The graphene oxide is used as the nanoscale substrates for the nanocomposite formation with different metal oxides. The nanocomposite of graphene/TiO_2 can also induce visible light activity by extending the excitation wavelength to longer wavelengths [23-24].

Nitrophenols can be present in industrial wastewater, in particular, 4-nitrophenol and its derivatives result from the production processes of pesticides, herbicides and synthetic dyes [25-26]. These pollutants have high toxicity and carcinogenic character. Chromium exhibits variable valencies of which Cr(III) and Cr(VI) forms are common. The behaviour of Cr-species depends strongly on its oxidation state. Cr (VI) is mobile and highly toxic where as Cr (III) is mostly immobile and environment friendly [27]. Trivalent form of chromium plays an essential role in plant and animal metabolism, while hexavalent chromium is directly toxic to man, animals and plants. Also as the hexavalent form is more stable than trivalent, it can easily penetrate through the cell

membrane in case of animals and subsequently retains inside the cell forming stable complexes. Hexavalent form of chromium is 100 times more toxic than trivalent [28]. Out of the total world production of dyes, 15% is lost during the dyeing process and is released in textile effluents. Among the textile dyes, methylene blue (MB) is a brightly coloured blue cationic thiazine dye, which is used as an antidote for cyanide poisoning in humans, antiseptic in veterinary medicine and most commonly, in vitro diagnostic in biology, cytology, hematology and histology [29-30].

These pollutants which are present in the wastewater have caused considerable damage to the ecosystem and human health. The traditional wastewater treatment methods include activated carbon adsorption, chemical oxidation, biological digestion, chemical precipitation, reverse osmosis, ion exchange, foam flotation, electrolysis, etc. However, there are some limitations in each technique. Most of these methods require either high energy or large quantities of chemicals, so there is a need of method which will be cost effective and more efficient for degradation of these pollutants. The photocatalytic process is found to be superior to all.

The significance of the present study is to find out the effect of graphene support towards the photocatalytic activity of sulfated nano TiO_2 particles. The novelty of the present study is the simple in-situ method of synthesis of graphene supported sulfated TiO_2 nano particles by simultaneous chemical reduction of graphene oxide and deposition of nano particles over the graphene layer. To know the effect of improvement of photocatalytic activity we have compared it with sulfated nano TiO_2 catalyst for the reduction of hexavalent chromium.

2. EXPERIMENTAL

2.1 Materials

Hydrated titania was prepared by sol–gel method taking tetraisopropyl orthotitanate (Fluka, 98%) as the starting material. In a typical preparation procedure, 50 mL of tetraisopropyl orthotitanate was dissolved in 400 mL of isopropanol (Qualigens, 99.7%), and to this solution 12.7 mL of distilled water at pH 3.0 (1 M H_2SO_4) was added drop wise under vigorous stirring. The resulting colloidal suspension was stirred for 3 h and aged at 80◦C for 10 h. The gel obtained was filtered, washed, and dried at 100 ◦C for 12 h. A series of sulfated nanoTiO_2 samples with varying weight percentages of sulfate were prepared by an aqueous wetness impregnation method using H_2SO_4. The suspended mass was evaporated to dryness on a hot plate with constant stirring. The samples were dried in an air oven at 100 ◦C and subsequently activated at 400 ◦C at a heating rate of 10◦C/min in a muffle furnace for 4 h.

Graphene supported sulfated nano TiO_2 composite were prepared by chemical reduction method taking graphene oxide (prepared by Hummers method) and 2.5 wt% sulfated nanoTiO_2. In a typical method of synthesis, calculated amount of graphene oxide was sonicated for 30 min to which 0.5 g of sulfated nanoTiO_2 was added and stirred over a magnetic stirrer. The mixture was stirred for 30 min, then to this cold solution, sodium borohydride was added and the solution was further stirred for 30 minutes. After that it was filtered, washed repeatedly with distilled water and finally dried in an oven for further use. The samples prepared for this work are 5 wt% and 10 wt% graphene promoted sulfated nano TiO_2 (5 RGO-S/TiO_2 and 10 RGO-S/TiO_2)

2.2 Characterisation

To determine the crystal phase composition of the catalyst, powder X-ray diffraction (PXRD) was carried out on a Philips X-ray diffractometer. The specific surface area (BET) of the catalysts was measured by N_2 adsorption–desorption studies at liquid nitrogen temperature (−196 ◦C) using Quantasorb (Quantachrome, USA). Prior to the analysis, samples were degassed at 200◦C. FTIR spectra of the samples were recorded in a Varian FTIR spectrophotometer (FTS-800) in the range of 400–4000 cm^{-1} taking KBr as the reference. The high resolution TEM images were obtained using a JEOL 2010 electron microscope with a LaB_6-cathode operated at a voltage of 200 kV. The samples for electron microscopy were prepared by dispersing the powder in ethanol and coating the very dilute suspension on carbon coated Cu grids. TEM images were recorded by using Gatan CCD camera. The particle sizes were determined by using several TEM micrographs. PL spectra were recorded in Perkin Elmer Fluorescence spectrometer (LS55).

2.3. Photocatalytic reaction

The solutions were exposed to sunlight with constant stirring. All the irradiation was performed in triplicate during sunny days, from 10:00 a.m. to 3:00 p.m., when the average solar intensity was 0.80 kW/m^2 and the intensity fluctuations were minimal.

The photocatalytic degradation of 4-nitrophenol (4-NP) was performed taking 0.05 g/L of substrate. The pH of the dispersion was adjusted by addition of dilute sulphuric acid. The solutions were exposed to sunlight in closed Pyrex flasks (no extra cooling) with constant stirring. The corresponding dark controls were

carried out simultaneously for comparison. After irradiation at different time intervals, the suspension was filtered and 4-nitrophenol was analysed quantitatively by measuring the absorption at 315 nm using Cary-1E (Varian) spectrophotometer. The detail method for measurement was available in [31].

The photocatalytic reduction of hexavalent chromium {Cr(VI)} was performed with 20 ppm Cr(VI) solution. Blank experiment was carried out taking dichromate solution without photocatalyst to know the extent of reduction of hexavalent chromium concentration due to solar radiation. After irradiation and also adsorption, the suspension was filtered and the Cr(VI) content was analysed quantitatively by measuring the absorption band at 348 nm using Cary-1E (Varian, Australia) spectrophotometer [32].

The decolorization of methylene blue (MB) was performed taking 25mL of 100 ppm solution in pyrex flask. After reaction, the suspension was centrifuged to separate the catalyst and MB concentration was analysed quantitatively by measuring the absorption band at 665 nm using Cary-1E (Varian, Australia) spectrophotometer. All the chemicals used in these experiments are of Analytical Grade and are used without further purification.

3. RESULTS AND DISCUSSION

3.1 Characterization

3.1.1. Characterization of sulfated nano TiO_2.

The nano TiO_2 samples were synthesized using organic precursor at pH 3. The acidic condition in the hydrolysis process prevents agglomeration of the particles synthesized; there by the size of the particles formed are around 12 nm.

The XRD pattern reveals the presence of both anatase and rutile phases in neat TiO_2, whereas only the anatase phase is present in sulfated nano TiO_2. From this result, we believed that sulfate modification probably stabilizes the anatase phase and inhibits the phase transformation. It is observed that the crystallite size of titania decreases with sulfate loading. In addition to stabilizing anatase TiO_2 crystallites, sulfate species inhibit TiO_2 crystallite sintering, leading to smaller crystallites. The crystallite size decreases in the presence of sulfate ions, as SO_4^{2-} species could possibly interact with the TiO_2 network, and thus hinder the growth of the crystal. Even a very small amount of SO_4^{2-} species is sufficient for this effect. Therefore, it is assumed that a small amount of sulfate species is responsible for the lowering of crystallite size. Therefore, the change in sulfate concentration did not change crystallite size further. Among a series of sulfate modified TiO_2 samples (2.5 wt%, 5 wt%, 7.5 wt% and 10 wt%), 2.5 wt% TiO_2 exhibits the highest activity. So in the present investigation we have made detail characterization of 2.5 wt% sulfate loaded TiO_2 [33]. The N_2 adsorption–desorption isotherms and the pore size distribution of neat TiO_2 and 2.5 wt% sulfated nanoTiO_2 samples show type IV isotherm and an H1 hysteresis loop, which clearly indicates the mesoporous nature of TiO_2. Sulfate modification leads to increased in surface area, pore size, and pore volume of the catalyst. The relatively high surface areas of sulfate-modified samples as compared to neat samples confirms that the frameworks of mesoporous TiO_2 have better thermal stability due to the stabilizing effect of sulfate ions. The increase in pore size and pore volume after sulfate modification is due to the progressive coalescence of small pores to form large pores. This implies that the presence of sulfate plays a role in making the material porous. The presence of low amount of sulphate ion may be responsible in the formation of porous network, due to changes in the Ti---O---Ti bond strength by the attachment of sulphate bridges. The FTIR spectra of pure TiO_2 and sulfated nanoTiO_2 are showing the peak corresponding to 1375 cm^{-1} for the stretching frequency of S=O, and the peaks corresponding to 1131 and 1044 cm^{-1} are the characteristic frequencies of sulfate ion. The peaks at 436 and 495 cm^{-1} for pure TiO_2 and 476 cm^{-1} for sulfated nanoTiO_2 are contributions from the vibration modes of anatase skeletal O–Ti–O bonds. The broad absorption band in the region of 3200–3400 cm−1 is characteristic of the OH stretching vibration of surface hydroxyl groups and the peak corresponding to 1630 cm^{-1} has been assigned to H–O–H bending of physically adsorbed water [34].

3.1.2: Characterization of graphene-sulfated nanoTiO_2 composites

Figure 1 (a) shows the XRD pattern of graphene oxide (GO) having a strong [001] reflection peak at 2θ ~10°. We observed that [001] reflections of GO is not found for the graphene supported sulfated TiO_2 nanocomposite as seen in figure 1 (b). The pattern shows a strong peak at 2θ ~ 25.3 °, which is the characteristic peak for the anatase phase of TiO_2.

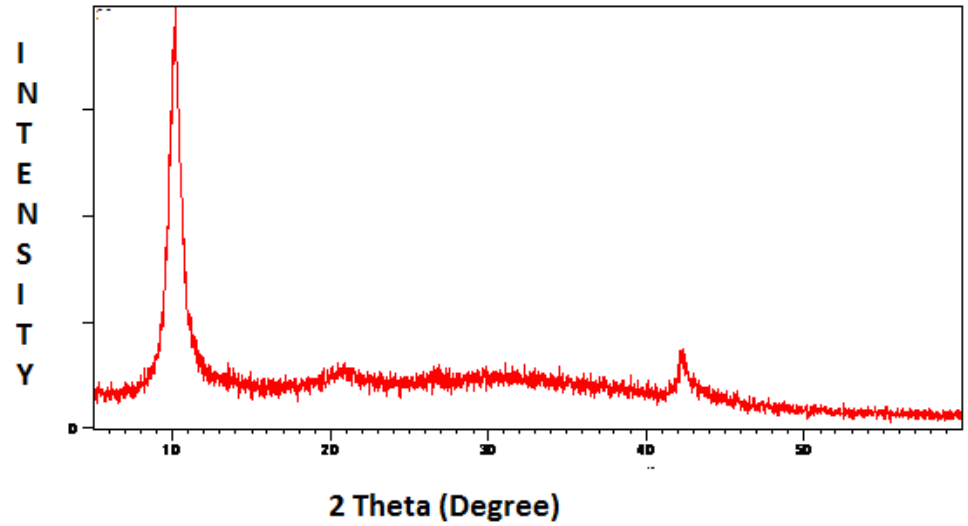

Figure 1. (a). XRD pattern of graphene oxide sheets

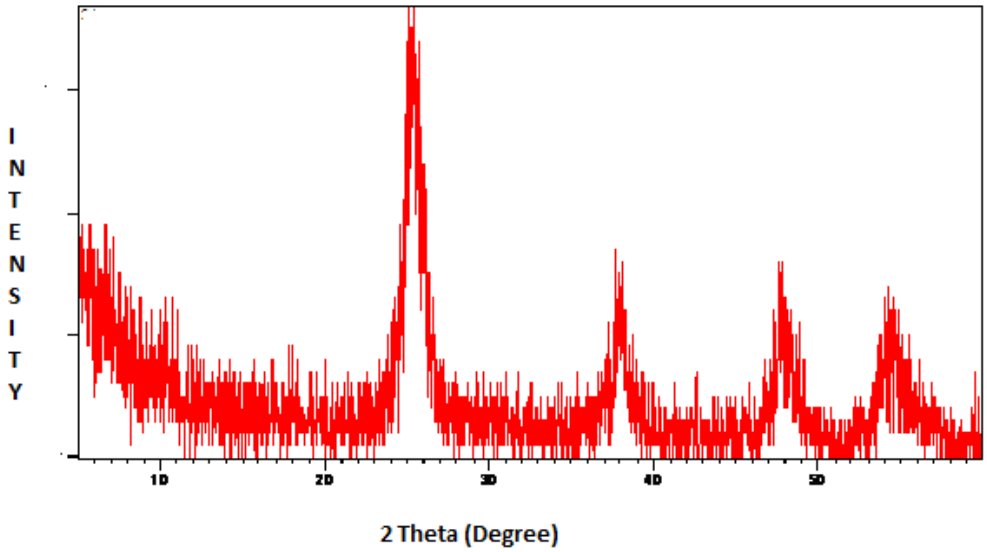

Figure 1. (b). XRD Pattern of graphene-sulfated nanoTiO$_2$ nanocomposite

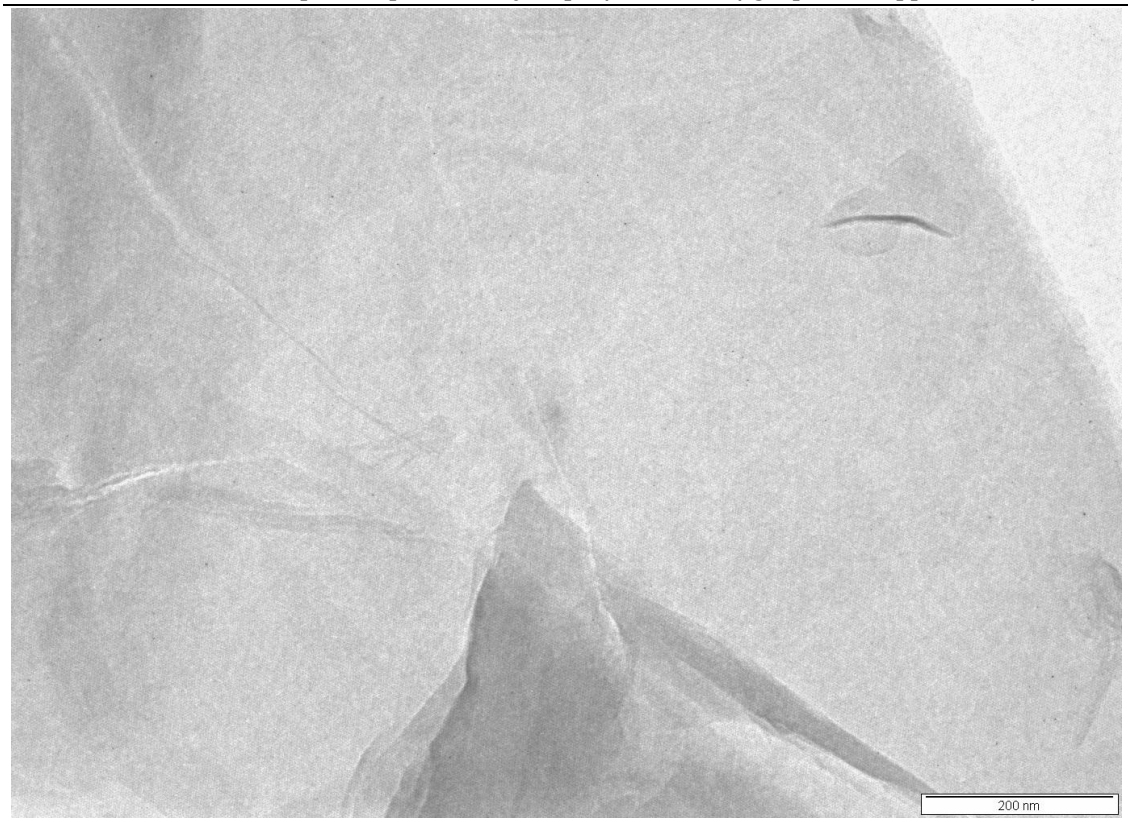

Figure 2. (a). TEM image of RGO sheet

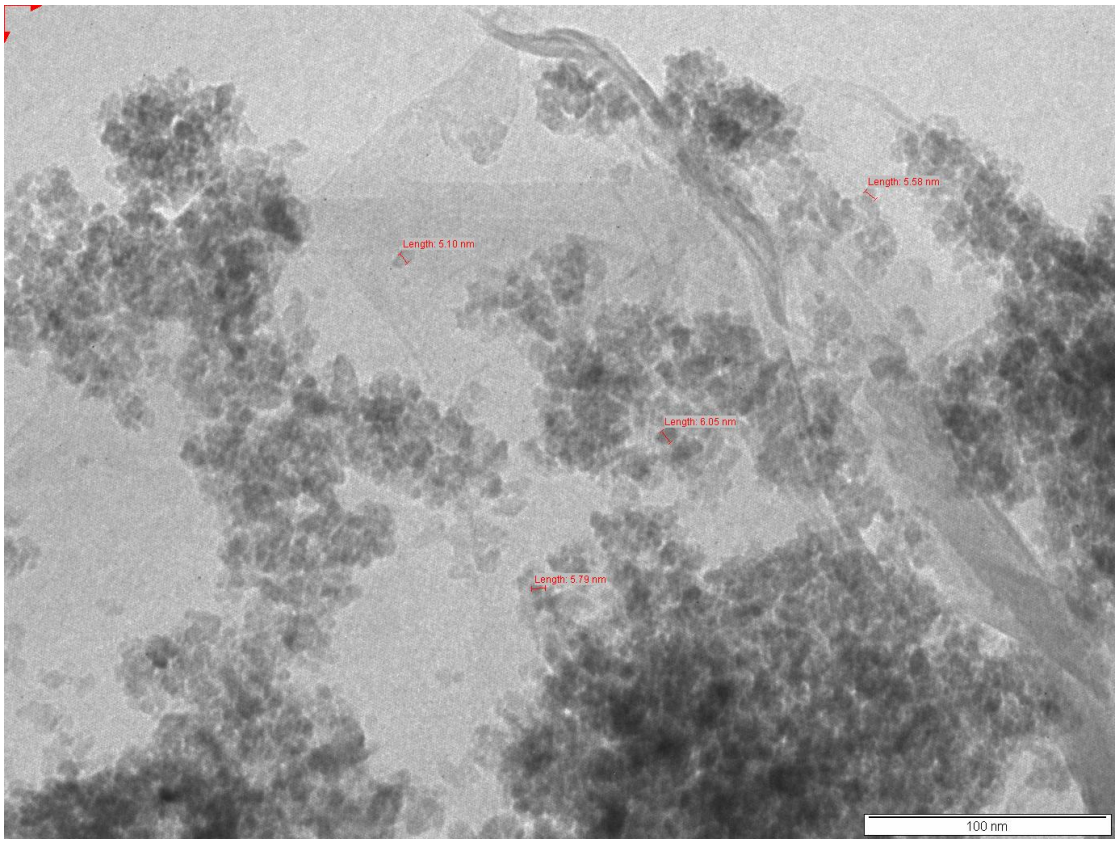

Figure 2. (b). TEM image of graphene supported sulfated nanoTiO_2 composite

The TEM images of reduced graphene oxide (RGO) and graphene-sulfated nanoTiO_2 composite are shown in figure 2. (a) and (b), respectively. The morphology of RGO, consisting of thin well defined few layer

structures at the edge, as clearly seen in fig. 2 (a). The nanocomposite reveals a homogeneous dispersion of nano particles of sulfated TiO_2 in the RGO matrix. It seems sulfated TiO_2 nanoparticles having average size of 5-6 nm are entrapped possibly inside the RGO sheets.

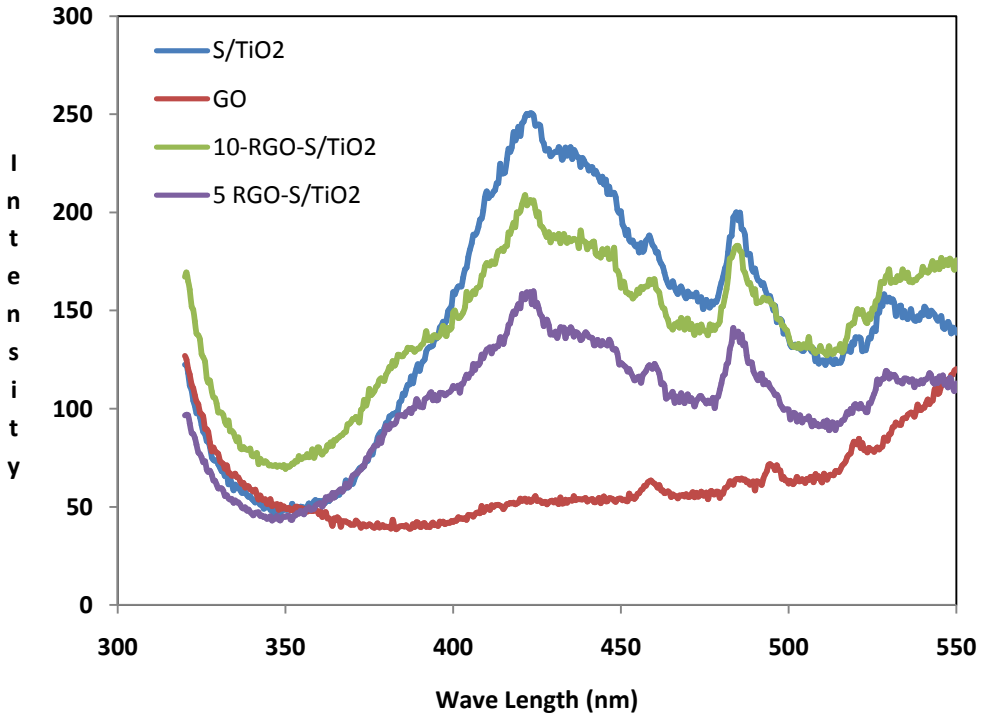

Figure-3 PL spectra of Sulfated nano TiO_2 and graphene-sulfated nano TiO_2 composite

Photoluminescence (PL) emission spectra analysis used to investigate the efficiency of charge carrier trapping, immigration and transfer to predict the fate of electron-hole pairs in semiconductor particles [35]. Figure 3 shows the PL spectra of all samples excited at wave length of 300nm. We observed two peaks at about 424 and 484 in the regions (400 - 500 nm). These may be attributed to the emission of the band gap transition. We observed that the PL spectra of sulfated nanoTiO_2 have higher intensity; the graphene supported sulfated nanoTiO_2 composites possess nearly similar pattern, but having less intensity. This result demonstrates that the recombination of electron and hole is inhibited by the presence of graphene. The 5 wt % graphene-sulfated nanoTiO_2 composite has much less intensity than parent sulfated nano TiO_2, so its photocatalytic activity is much better. Graphene being a good electron acceptor favors the transfer of the photo-generated electrons from the conduction band of TiO_2 to the graphene sheet, there by enhance the charge separation efficiency thus prevent the recombination of the electron and hole [36-37].

3.2 Photocatalytic activity

3.2.1. Degradation of PNP, Cr (VI) and MB over sulfate modified nano TiO_2

Figure-4 shows the effect of solution pH on the percentage of degradation of pollutants. It is found that with increasing the pH of the solution, 4-nitrophenol degradation decreases gradually. Since no nitrobenzene was detected during the degradation of 4-nitrophenol at pH 2, it can be concluded that the reductive pathway is favoured in acidic media. It is known that nitro aromatic compounds such as 4-nitrophenol are reduced in acidic media more easily than in alkaline solutions [38]. We observed similar trend for reduction of Cr(VI). The highest reduction rate was obtained at the lower pH. This may be due to the transformation of dominant form of Cr (VI) at pH 2 i.e. $HCrO_4^-$ to CrO_4^- and $Cr_2O_7^{2-}$ with increase in pH. At pH above 7, the photocatalyst surface becomes negative and repels dichromate ion.

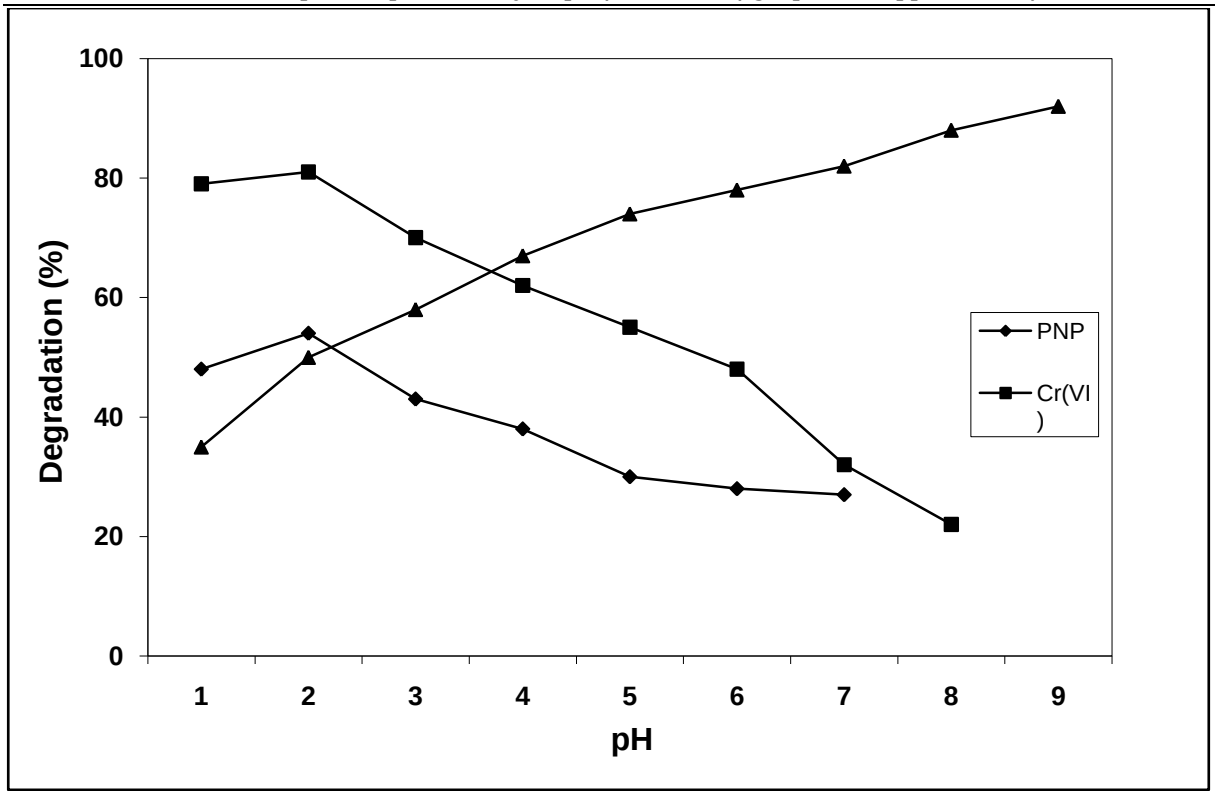

Figure 4: Effect of pH of solution on degradation percentage.

At pH above 7, neither adsorption nor reduction takes place; this type of observation is also reported by others [39, 40]. The specific adsorption of H^+ ions favours the approach of Cr (VI) species to the semiconductor surface, whereas at higher pH, excess of absorbed OH^- ions has the opposite effect, leading to low levels of Cr (VI) adsorption. For the MB decolorization, the percentage of decolorization increases with increasing the pH. So pH influences both the surface state of titania and the ionization state of ionizable organic molecule simultaneously [41]. The pH effect can be explained on the basis of zero point charge of TiO_2. The pH_{pzc} of TiO_2 is 3.5–6.7 [42]. At pH value higher than $pH_{pzc,}$ the surface becomes negatively charged and it is opposite for pH value less than pH_{pzc}. Since methylene blue is a cationic dye, at high pH the adsorption is favored on a negatively charged surface. Since the adsorption is a requirement for reaction, the reaction is faster at basic pH.

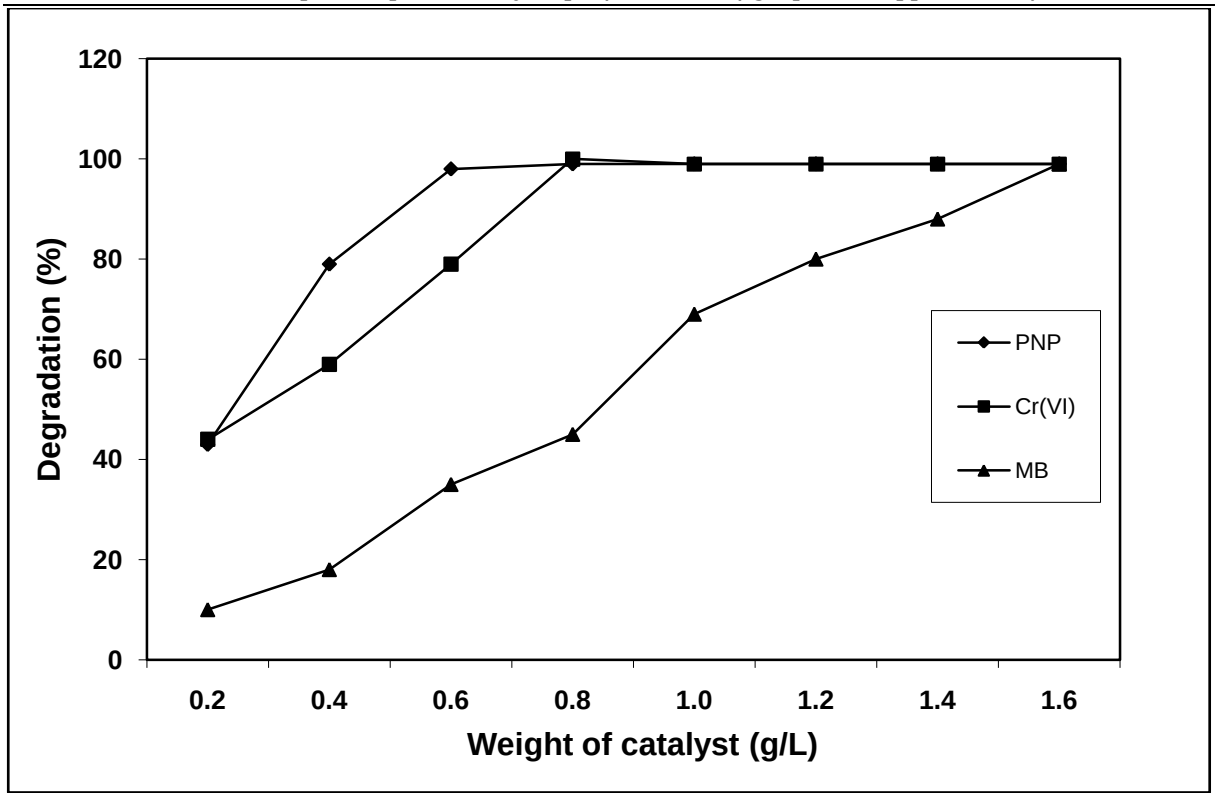

Figure 5: Effect of weight of catalyst on the degradation percentage

Figure-5 represents the effect of catalyst load on the degradation percentage of PNP, Cr (VI) and MB degradation. For the PNP degradation, 0.6 g/L of sulfated nano TiO_2 is sufficient for the concentration 0.05g/L. The Cr(VI) reduction requires 0.8g/L of catalyst for the complete reduction of 20 ppm in 3h. The MB decolourization reaction requires 1.6 g/L of catalyst for 100 ppm solution, which was found to be very effective compared with the reports available [43]. The catalyst load varies for the pollutants due to the nature of pollutant, adsorption of the pollutant on the surface of the catalyst and concentration of the pollutant.

Figure-6 shows the effect of time of the reaction for degradation process using sulfated nanoTiO_2 as the photocatalyst. Both the PNP and Cr(VI) requires 3h for the complete degradation process, where as 100 ppm MB requires 4 h for the complete decolorization reaction. The reason may be due to the type of the reactants and concentration of the pollutants under investigation.

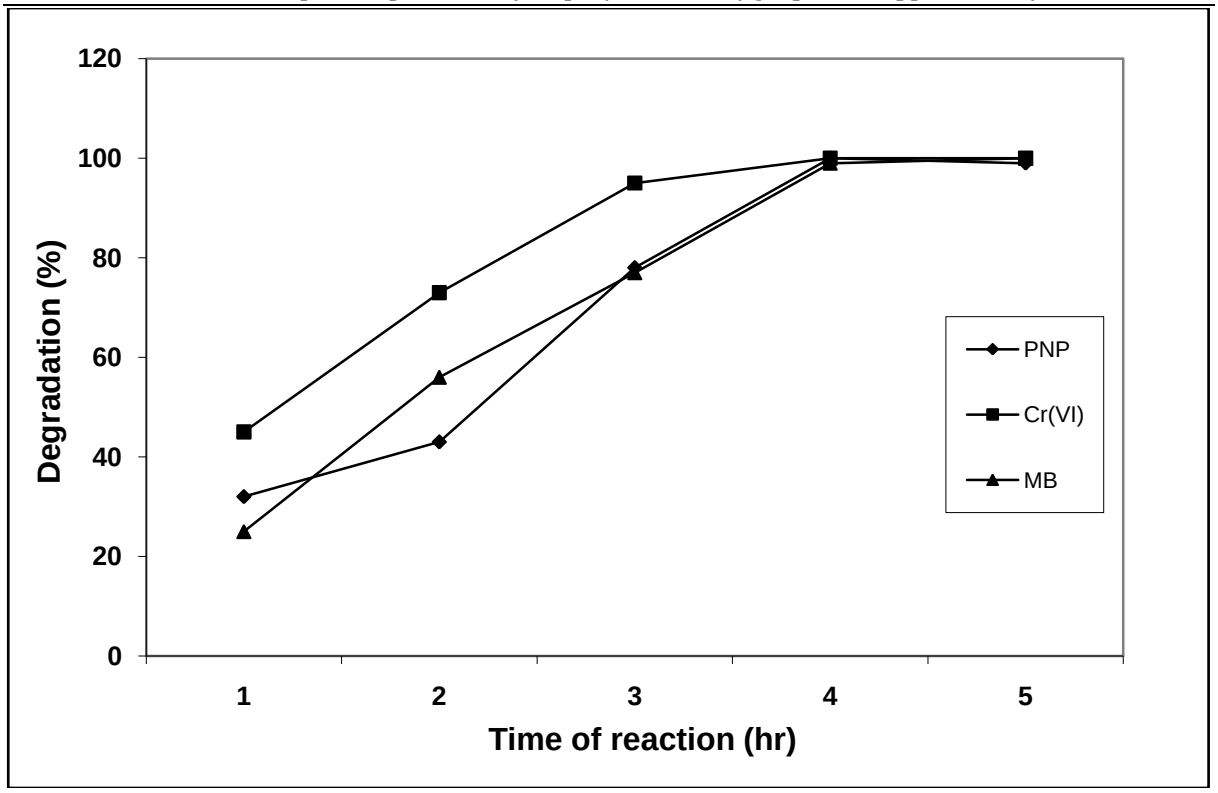

Figure 6: The effect of time of the reaction on degradation percentage

The incorporation of sulphate ion in the TiO_2 matrix affects the surface area, pore volume and pore size distribution which may be responsible for the increase in catalytic activity [36, 43-44]. We observed the decrease in photocatalytic activity at higher activation temperature, may be due to loss of porous structure of nanoparticles, formation of denser particles due to sintering as well as transformation into rutile from anatase phase. Addition of H_2O_2 and potassium persulfate to the methylene blue solution decreases the time for complete decolourization [43].

3.2.2. Photoreduction of Cr (VI) over graphene-sulfated nano TiO_2 composite

Graphene has been reported to be an electron acceptor material due to its two dimensional π conjugation structure. The application of graphene based composites in the area of solar energy conversion is topic of great interest. Reports are available on the application of graphene based materials for photocatalytic activity [36, 44-48]. Attentions have been focussed on the photodegradation of organic pollutants and photocatalytic hydrogen evolution using graphene/TiO_2 photocatalyst.

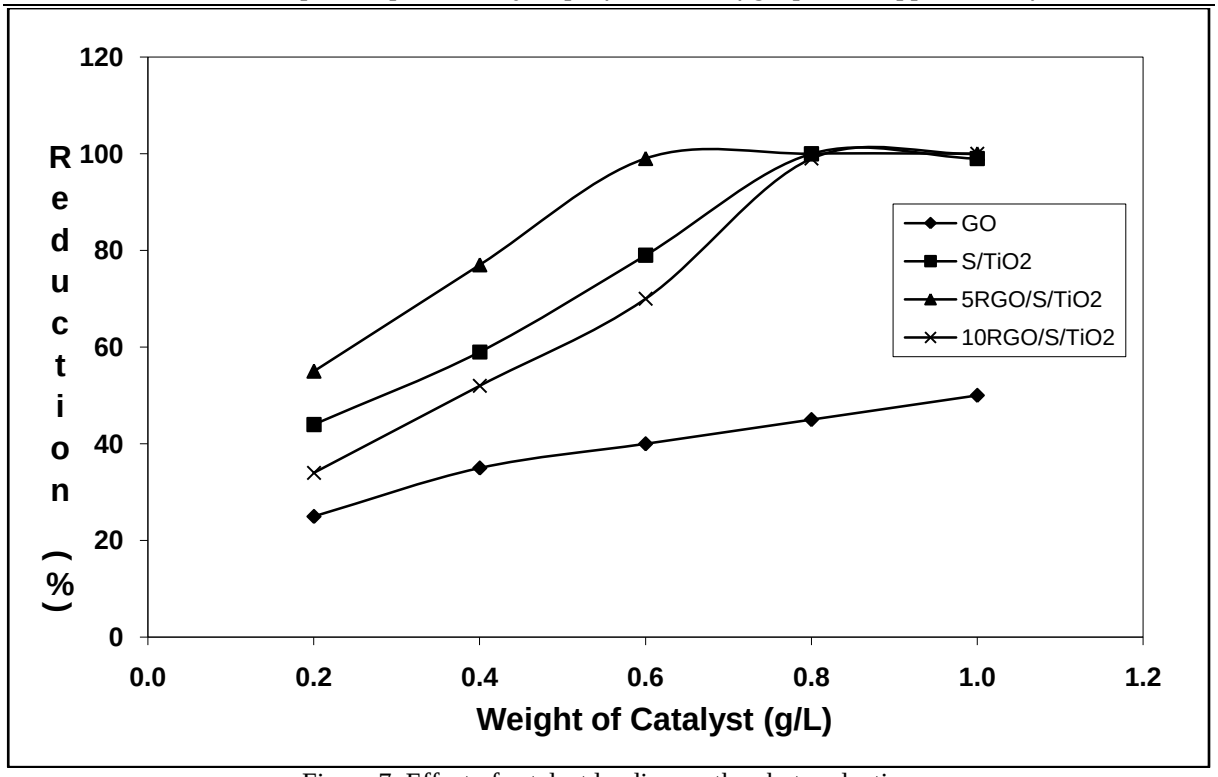

Figure 7: Effect of catalyst loading on the photoreduction

The photocatalytic reductions of hexavalent chromium over graphene supported sulfated nano TiO_2 composite were carried out at optimum experimental conditions used for sulfated nano TiO_2 photocatalyst. Figure 7 shows the effect of catalyst loading on the reduction process. We observed that the reduction ability of 10 wt% graphene sulfated nano TiO_2 phtotcatalyst is lower than the sulfated nano TiO_2. The 5 wt% graphene-sulfated nanoTiO_2 shows enhanced activity. The results were in agreement with our earlier studies for the photo-hydroxylation of phenol using RGO–Ag_3VO_4 nanocomposites [49] and the results obtained by X. Zhang et. al [50] for the H_2 evolution using TiO_2/graphene composites. The activity results are also supports the PL spectra of the highly active sample (5RGO-S/TiO_2).

4. Mechanism

The possible mechanism of the photoreduction of Cr(VI) over the graphene supported sulfated TiO_2 nano composite may be described by the following steps:

(i). Formation of electron-hole pair by the incident of photon of light.

(ii). The excited electron is transferred from nano TiO_2 to graphene sheet, which prevents the recombination process.

(iii). Cr(VI) ion captures the mobile electron from graphene sheets and reduced to Cr(III).

(iv). Water is oxidized by the holes.

$$RGO\text{-}S/TiO_2 + h\upsilon \rightarrow e^-_{(CB)} + h^+_{(VB)} \quad (1)$$

$$h^+_{(VB)} + H_2O(OH^-) \rightarrow OH^{\bullet} \quad (2)$$

$$CrO_4^{2-} + 8H^+ + 3e^-_{(CB)} \rightarrow Cr^{3+} + 4H_2O \quad (3)$$

$$2H_2O \rightarrow O_2 + 4H^+ + 4e^- \quad (4)$$

The net reaction is as follows

$$4CrO_4^{2-} + 20H^+ \rightarrow 4Cr^{3+} + 10H_2O + 3O_2 \quad (5)$$

The mechanism of reduction can be directly co-related with the size of the sulphated TiO_2 particles. Generally, titania photocatalysts with smaller particle sizes are more effective in the catalytic/photocatalytic reactions. Crystallinity is also important for high photoactivity. The charge recombination usually prevails for the titania photocatalysts with low crystallinity. Among the different phases of titania, the anatase phase is generally considered as the active phase for charge carrier dynamics [51] and chemical properties [52]. It is also reported that the charge carriers generated in anatase have longer lifetimes than those in rutile [53-54]. Our samples support the reported results in terms of the phase of the photocatalyst. Also due to the presence of the nano particles the adsorption efficiency increases thereby it improves the photoreduction.

The graphene supported sulfated nano TiO_2 was prepared by in-situ chemical method. The presence of carboxyl and epoxides helps it to be used in both polar and nonpolar solvents, thereby there is formation of uniform loading of the nano particles over the graphene sheets. Due to the in-situ reduction and deposition of the nano particles over the graphene sheets, there is efficient electron transfer between graphene and nono particles, which helps in the improvement of the photocatalytic property. In graphene-TiO_2 nanocomposite, the excited electron of TiO_2 could transfer from conduction band to graphene, thereby preventing the recombination thus enhances the photocatalytic reactions. The better photocatalytic properties on the graphene-sulfated nanoTiO_2 nanocomposite could be attributed to an increase in the absorption of visible light by narrowing the band gap of the nanocomposite compared to pure TiO_2 and effective charge transfer. Graphene modifications can be used for the synthesis of efficient photocatalysts for the degradation of pollutants present in water or wastewater system.

5. Conclusions

(i) The presence of sulfate ions as SO_4^{2-} species could possibly interact with TiO_2 network, and thus hinder the growth of the particle, stabilises the phase, increases the surface area and enhances the photocatalytic activity.
(ii) The photocatalyic activity of sulfated TiO_2 towards photoreduction of Cr(VI further improved when loaded with graphene sheets due to uniform distribution and strong interaction between graphene and nano particles.
(iii) The improved activity of sulphated nano TiO_2 supported on graphene sheets has been attributed to the enhanced surface, textural, electronic and optical properties of the nanocomposites.
(iv) The detailed study on the improved photoactivity of these nanocomposites has been going on in our group to have in-depth understanding.

Acknowledgments

The authors are thankful to Science and Engineering Research Board (SERB), Department of Science and Technology, Government of India, New Delhi for the financial assistance to carry the present work vide the sanction order no **SR/FT/CS-61/2011** Dated 16/05/2012 under Fast Track Scheme. We are very much thankful to SAIF (RSIC), I.I. T., Mumbai for their timely help in instrumental analysis (TEM, FTIR, etc).

References

[1]. R. Andreozzi, V. Caprio, A. Insola, R.Marotta, Catal. Today 53 (1999) 51.
[2]. J.-M. Herrmann, Catal. Today 53 (1999) 115.
[3]. G. Nayak, P. Misra and K. M. Parida, Chemical Engineering Journal, 229 (2013) 492.
[4]. S. Martha, D.P. Das, N. Biswal and K.M. Parida, J. Mater. Chem. 22 (2012) 10695
[5]. J. Cunningham, G. Al-Sayyed, P. Seldak, J. Caffrey, Catal. Today 53 (1999) 145.
[6]. O.M. Alfano, D. Bahnemann, A.E. Cassano, R. Dillert, R. Goslich, Catal. Today 58 (2000) 199.
[7]. N. Sahu and K. M. Parida, Kinet. Catal., 53 (2012) 197.
[8]. J.C. Yu, J. Yu, W. Ho, Z. Jhing, L. Zhang, Chem. Mater. 14 (2002) 3808.
[9]. K. M. Parida and N. Sahu, J. Mol. Catal A. Chem. 287 (2008) 151.
[10]. H. Yang, K. Zhang, R. Shi, X. Li, X. Dong, Y. Yu, J. Alloys Compd. 413 (2006) 302.
[11]. P. Mohapatra, T. Mishra and K.M. Parida Appl. Catal. A. Gen. 310 (2006) 183.
[12]. N. Guettai, H. Ati Amar, Desalination 185 (2005) 439.
[13]. Muggli, D. S.; Ding, L. F. Appl.Catal., B 32 (2001) 181.
[14]. Wang, X. C.; Yu, J. C.; Hou, Y. D.; Fu, X. Z. Adv. Mater. 107 (2005) 99.
[15]. Colon, G.; Hidalgo, M. C.; Navio, J. A. Appl. Catal., B 45 (2003) 39.
[16]. Wang, X. C.; Yu, J. C.; Liu, P.; Wang, X. X.; Su, W. Y.; Fu, X. Z. J. Photochem. Photobiol., A 179 (2006) 339.
[17]. Xu, Y. H.; Wang, L. Y.; Zhang, Q.; Zheng, S. J.; Li, X. J.; Huang, C. Mater. Chem. Phys. 92 (2005) 470.
[18]. Nakajima, A.; Obata, H.; Kameshima, Y.; Okada, K. Catal.Commun. 6 (2005) 716.
[19]. K.S. Novoselov, A.K. Geim, S.V. Morozov, D. Jiang, Y. Zhang, S.V. Dubonos, I.V.Grigorieva, A.A. Firsov, Science 306 (2004) 666.
[20]. V.H. Luan, H.N. Tien, T.V. Cuong, B.-S. Kong, J.S. Chung, E.J. Kim, S.H. Hur, J. Mater. Chem. 22 (2012) 8649.
[21]. Z. Fan, K. Wang, T. Wei, J. Yan, L. Song, B. Shao, Carbon 48 (2010) 1686.
[22]. M.J. Allen, V.C. Tung, R.B. Kaner, Chem. Rev. 110 (2009) 132.
[23]. A.K. Geim, K.S. Novoselov, The rise of graphene, Nat. Mater. 6 (2007) 183.
[24]. Q. Xiang, J. Yu, M. Jaroniec, Chem. Soc. Rev. 41 (2012) 782.

[25]. Y. Liu, Y. Hu, M. Zhou, H. Qian, X. Hu, Appl. Catal. B 125 (2012) 425.
[26]. M.S. Dieckmann, K.A. Gray, Water Res. 30 (1996) 1169.
[27]. N. Takahashi, T. Nakai, Y. Satoh, Y. Katoh, Water Res. 28 (1994) 1563.
[28]. J. Kotas, Z. Stasicka, Environ. Pollut. 107 (2000) 263.
[29]. C. Franc¸oise, A. Richard, C.M. Bourg, Water Res. 25 (1991) 807.
[30]. Aldrich Handbooks of Dyes and Strains, Aldrich Chemicals, 1996, p. 448.
[31]. K.G. Bhattacharya, A. Sharma, Dyes Pigments 65 (2005) 51.
[32]. V. Augugliaro, L. Palmisano, M. Schiavello, A. Sclafani, L.Marchese, G. Martra, F. Miano, Appl. Catal. A: Gen. 69 (1991) 323.
[33]. G. Colon, M.C. Hindalgo, J.A. Navio, Appl. Catal. A: Gen. 231 (2002) 185.
[34]. S. K. Samantaray, P. Mohapatra, K. M. Parida, Journal of Molecular Catalysis A: Chemical 198 (2003) 277.
[35]. K.M. Parida, N. Sahu, N.R. Biswal, B. Naik, A.C. Pradhan, Journal of Colloid and Interface Science 318 (2008) 231.
[36]. J-G. Yu, H-G. Yu, B. Cheng, X-J. Zhao, J. C. Yu and W-K. Ho, Journal of. Physical Chemistry B. 107 (2003)13871.
[37]. G. Liao, S. Chen, X. Quan, H. Yu and H. Zhao, J. Mater. Chem., 22 (2012) 2721.
[38]. S. Pany, K. M. Parida and B. Naik, RSC Advances 3 (2013) 4976.
[39]. R. Dillert, I. Fornefett, U. Siebers and D. Bahnemann, J. Photochem. Photobiol. A: Chem. 94 (1996) 231.
[40]. J. Munoz and X. Domenech, J. Appl. Electrochem. 20 (1990) 518.
[41]. Y. Guo, J. Qi, S. Yang, K. Yu, Z. Wang and H. Xu, Mater, Chem. Phys. 78 (2002) 132.
[42]. C. Guillard, H. Lachheb, A. Houas, M. Ksibi, E. Elaloui and J.-M. Herrmann, J. Photochem. Photobiol. A: Chem. 158 (2003) 27.
[43]. S. Lakshmi, R. Renganathan and S. Fujita, J. Photochem. Photobiol. A: Chem. 88 (1995) 163.
[44]. P. Mohapatra and K. M. Parida, Journal of Molecular Catalysis A: Chemical 258 (2006) 118–123.
[45]. A.P. Rivera, K. Tanoka and T. Hisanaga, Appl. Catal. B: Environ. 3 (1993) 37.
[46]. B. Liu, Y. Huang, Y. Wen, L. Du, W. Zeng, Y. Shi, F. Zhang, G. Zhu, X. Xu and Y. Wang, J. Mater. Chem 22 (2012) 7484.
[47]. G. Zhao, T. Wen, C. Chen and X. Wang, RSC Advances, 2 (2012) 9286
[48]. J. Zhang, Z. Xiong and X. S. Zhao, J. mater. Chem., 21 (2011) 3634
[49]. D. P. Das, R. K. Barik, J. Das, P. Mohapatra and K. M. Parida, RSC Advances, 2 (19), 2012, 7377.
[50]. X. Zhang, H. Li, X. Cui and Y. Lin, J. Mater. Chem., 20 (2010) 2801.
[51]. T. Sumita, T. Yamaki, S. Yamamoto, A. Miyashita, Appl. Surf. Sci. 200 (2002) 21–26.
[52]. T. Torimoto, N. Nakamura, S. Ikeda, B. Ohtani, Phys. Chem. Chem. Phys. 4 (2002) 5910–5914.
[53]. C. Colbeau-Justin, M. Kunst, D. Huguenin, J. Mater. Sci. 38 (2003) 2429–2437.
[54]. Gonghu Li a, Le Chena, Michael E. Grahamb, Kimberly A. Gray, J. Molecular Catal A: Chemical 275 (2007) 30–35